

# Fracture detection using $P$ - $P$ and $P$ - $S$ waves in multicomponent sea-floor data

Xiang-Yang Li, Edinburgh Anisotropy Project, British Geological Survey

## Summary

The azimuthal variations in  $P$ - $P$  amplitude, velocity, and interval moveout show elliptical variations in azimuthally anisotropic media. This can be used to determine the fracture strike of the medium and has been verified from real data. However, the  $P$ -wave effects only occur at sufficiently large offsets with multi-azimuths, and are often complicated by other factors. This limits the application of  $P$ -wave analysis to some extent. Analysis of  $P$ - $S$  waves may thus prove to be beneficial. For near vertical propagating  $P$ - $S$  waves, the polarization and time delay of the shear-wave provide a direct measurement of the fracture orientation and intensity. The fracture strike (polarization azimuth) is diagnosed by a polarity change and amplitude dimming in the azimuthal gathers of the transverse-geophone component. Based on this, a robust method is presented for recovering the fracture strike using a 3D cross geometry where the source boat sails across the receiver cable.

## Introduction

Recently, the use of  $P$ -waves has attracted considerable interest because of their relatively low cost in acquisition. These uses include azimuthal  $P$ -wave AVO (Lynn *et al.* 1996 and Mallick *et al.* 1996), and azimuthal variations in  $P$ -wave NMO velocity (Sena 1991 and Tsvankin 1995), and interval moveout (Li 1997). With the advent of multicomponent sea-floor seismic technology, the study of mode converted shear-waves has become increasingly common in the industry. The mode-converted  $P$ -to- $S$  wave retains the benefit of both  $P$ - and  $S$ -wave surveys (Li *et al.* 1996) and offers the potential for more cost-effective reservoir characterization and monitoring.

Here, assuming fracture-induced transverse anisotropy with a horizontal symmetric axis (TIH), which is the simplest form of azimuthal anisotropy, I review and compare the  $P$ - $P$  and  $P$ - $S$  processing methods for determining the fracture strike and intensity from multicomponent sea-floor data. For  $P$ -wave processing, I will discuss azimuthal variations in amplitude, NMO velocity and interval moveout based on analytical approximate expressions for weak anisotropy. For  $P$ - $S$  wave processing, I will present new techniques for anisotropy analysis for a 3D crossline geometry where the source boat sails across the receiver cable (Figure 1). The technique and concept presented here can also be used for marine crossed 2D/3D surveys of different vintages, and for walkaway and 3D VSPs.

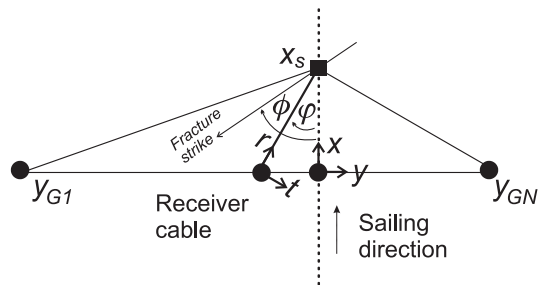


Figure 1. A plan view of a 3D cross geometry.  $(x, y)$  is the acquisition coordinate system;  $(r, t)$  is the local system associated with source-receiver azimuth  $\varphi$ ;  $\phi$  is the fracture strike measured from the boat direction  $x$ .

## Azimuthal $P$ -wave analysis

$P$ -wave amplitude and velocity. For a fixed offset with incidence angle larger than  $15^\circ$ , the reflection amplitude as a function of source-receiver azimuth ( $\varphi$ ) has the following form:

$$R_{pp}(\varphi) = A + B \cos 2\varphi, \quad (1)$$

where  $A$  and  $B$  are constants. Mallick *et al.* (1996) first presented equation (1) as an empirical expression from numerical modelling, and applied it to 3D land data to quantify fracture strike. Ruger (1996) provided an analytical account of the amplitude variation. Equation (1) forms the basis for azimuthal  $P$ -AVO analysis.

For a single reflector, the shot spread normal moveout velocity  $v_{nmo}$  for a given ray at azimuth  $\varphi$  can be written as,

$$\begin{aligned} v_{nmo}^2(\varphi) &= v_{p0}^2 [1 + 2(\delta - 2\epsilon) \sin^2 \varphi] \\ &= C + D \sin^2 \varphi, \end{aligned} \quad (2)$$

where  $v_{p0}$  is the vertical  $P$ -wave velocity, and  $\epsilon$  and  $\delta$  are the Thomsen parameters (Thomsen 1986). This leads to,

$$v_{nmo}^2(\varphi) = v_{nmo}^2(0) \cos^2 \varphi + v_{nmo}^2(90^\circ) \sin^2 \varphi. \quad (3)$$

Equation (3) reveals a simple elliptical variation of the NMO velocity along the azimuthal direction. Grechka and Tsvankin (1996) generalized equation (3) for generally inhomogeneous anisotropic media, and Corrigan *et al.* (1996) applied equations (2) and (3) to real data.

## Fracture detection using $P$ - $P$ and $P$ - $S$ waves

**$P$ - $P$  interval moveout.** Assume a fractured layer with azimuthal anisotropy overlain by a weakly anisotropic overburden. Consider two orthogonal line-azimuths at angles  $\phi$  and  $\phi + \pi/2$  to the fracture strike, respectively (Lines 1 & 3, Figure 2). The azimuthal difference of the interval moveout for the fractured layer between these two lines also shows a  $\cos 2\phi$  variation (Li 1997)

$$\Delta t(\phi, x) = E(x, \epsilon, \delta) \cos 2\phi, \quad (4)$$

where  $E$  is a function related to the acquisition geometry and the fractured layer.

Consider another pair of orthogonal lines separated by an angle  $\varphi_0$  from the first pair (Lines 2 & 4, Figure 2), yielding

$$\tan 2\phi = \frac{(\Delta t_2 - \cos 2\varphi_0 \Delta t_1) / \sin 2\varphi_0}{\Delta t_1}, \quad (5)$$

where  $\Delta t_1 = \Delta t(\phi, x)$ , and  $\Delta t_2 = \Delta t(\phi + \varphi_0, x)$ . Denote the numerator in equation (5) as  $\Delta t'_2$ . Thus, for the four line configuration in Figure 2, the cross plot of  $\Delta t_1$  versus  $\Delta t'_2$  shows a linear trend, indicating the direction of  $2\phi$ . A least square analysis of the cross-plot can be used to estimate the fracture strike as,

$$\phi = \frac{1}{4} \tan^{-1} \left\{ \frac{2 \sum_x \Delta t_1 \Delta t'_2}{\sum_x (\Delta t_1^2 - \Delta t'^2_2)} \right\}. \quad (6)$$

Li (1998) applied this method to real data.

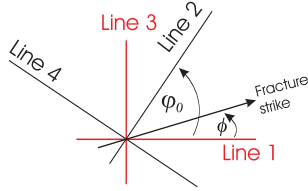


Figure 2. Four-line configuration.

### $P$ - $S$ polarization analysis

For near vertical propagation, the fast shear-wave ( $S1$ ) polarises parallel to the fracture strike, and the slow wave ( $S2$ ) polarises perpendicular to the strike (Figure 3). Furthermore the normalised time-delay between  $S1$  and  $S2$  satisfies:

$$\epsilon_{td} = \frac{t_2 - t_1}{t_1} = \gamma - \frac{1}{2} \epsilon_{td}^2 \approx \gamma, \quad (7)$$

where  $t_1$  and  $t_2$  are the interval travel times of  $S1$   $S2$ , respectively, for the fractured layer, and  $\gamma$  is the Thomsen parameter which is directly related to the fracture intensity. Thus  $P$ - $S$  wave polarization analysis provides an effective way to determine the fracture strike and density. For a conventional 2D acquisition, standard two-component rotation analysis for land shear-waves may be used to recover the polarization azimuth (Donati and Brown 1995).

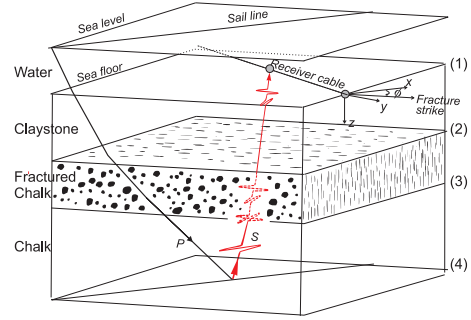


Figure 3. A four-layer model showing converted shear-waves in 3C sea-floor seismic acquisition over fractured media. A conversion at the reflection point is assumed. Numbers (1), (2), (3) and (4) mark the interface numbers.

For the cross geometry in Figures 1&3, a two-stage procedure can be used for anisotropy analysis. The first stage is to use the azimuthal gathers from crossline-shooting to estimate the polarization azimuth, and the second stage is to use the inline-shooting gathers to estimate the time delay of the split shear-waves. Full-wave modelling by the reflectivity method (Taylor 1990) for the model in Figure 3 and Table 1 will be used to verify the procedure. One crossline shooting gather (source offset  $x_s=1\text{km}$ , Figure 4) and one inline-shooting gather ( $x_s=0$ , Figure 5) are generated. Details of the method are outlined below.

Table 1. Layer parameters used in the study.

Layers	$\rho(\text{g/cm}^3)$	$v_p(\text{m/s})$	$v_s(\text{m/s})$	$\Delta z(\text{m})$
Water	1.00	1500	-	100
Claystone	1.97	1990	1000	1200
Fr. chalk*	2.2	3500	1750	300
Chalk	2.1	3080	1540	700
Clastic	2.37	4200	2100	-

$\Delta z$ =thickness

Fr. chalk\*=fractured chalk with 10% anisotropy

### Azimuthal variation of *P-S* amplitude

Consider the geometry in Figure 1. For the source-receiver azimuth  $\varphi$ , the horizontal components  $V_r$  and  $V_i$  in the local coordinate system  $(r, t)$  can be written as, for shear-waves only,

$$\begin{pmatrix} V_r(t_0, \Delta) \\ V_i(t_0, \Delta) \end{pmatrix} = \mathbf{R}^T(\Delta) \begin{pmatrix} \lambda_1(t_0) & 0 \\ 0 & \lambda_2(t_0) \end{pmatrix} \times \mathbf{R}(\Delta) \begin{pmatrix} PS(t_0) \\ 0 \end{pmatrix} \quad (8)$$

where  $t_0$  is time after *P-S* conversion,  $\Delta = \phi - \varphi$  is the angle between the fracture strike and the source-receiver azimuth,  $\mathbf{R}$  is a 2D rotation matrix,  $\lambda_1$  and  $\lambda_2$  are propagating functions for the fast and slow wave, respectively, and  $PS(t)$  is the effective shear-wave source due to conversion. It follows that,

$$\begin{aligned} V_i(t_0, \Delta) &= 0 \quad \text{for } \Delta = 0, \text{ or } \pi/2 \\ V_i(t_0, -\Delta) &= -V_i(t_0, \Delta). \end{aligned} \quad (9)$$

This implies that when the source-receiver azimuth is parallel, or perpendicular to the fracture strike, the energy in the transverse component vanishes, and that the wave forms show a polarity change.

Thus, an effective scheme can be used to determine the polarization azimuth based on these two criteria: polarity reversal and minimum amplitude,

- 1) sorting data into azimuthal gathers (Figures 4a&4b);
- 2) rotating the horizontal components by  $\varphi$  into the local coordinate system  $(r, t)$  (Figure 4c&4d)
- 3) determining the polarization azimuth  $\phi$  by applying the polarity reversal and minimum amplitude criteria (Figure 4d);
- 4) rotating the inline-shooting gathers by angle  $\phi$  to separate the fast and slow shear-wave and to determine the time delays (Figure 5).

The polarization azimuth is determined at  $30^\circ$  using this method for Figure 4d. The fast and slow shear-waves are clearly separated in Figures 5c&5d after rotating the inline gathers in Figures 5a&5b by  $30^\circ$ . Approx 20ms of time delay can be identified for the converted waves beneath the fractured chalk

(PS3, PS4, SS3, Figures 5c&5d), indicating about 10% anisotropy.

### Conclusions

For *P-P* wave analysis, the azimuthal variations in *P-P* amplitude, velocity, and interval moveout show elliptical variations in azimuthally anisotropic media. This can be used to determine the fracture strike of the medium. The use of azimuthal interval moveout has some distinct features. The method, based on a four-line configuration, utilises cross-plot analysis, and reveals good potential for effective compensation for the overburden anisotropy through the alignment of the top target reflections.

For *P-S* wave analysis, the *S1* polarization azimuth is parallel to the fracture strike, and the time delay between *S1* and *S2* is proportional to the fracture intensity for near-vertical propagations. A polarity reversal and amplitude dimming will occur in the azimuthal gathers of the transverse components. This feature provides robust and accurate estimates of the fracture strike using a 3D cross geometry where the source boat sails across the receiver cable. The time delay can be estimated from the inline shooting gather after separating the fast and slow waves.

### Acknowledgement

I thank Jianxin Yuan for help with the diagrams. This work is supported by the Edinburgh Anisotropy Project (EAP), and is published with the approval of the Director of the British Geological Survey (NERC), and the sponsors of EAP: Amerada Hess, Amoco, BG plc, Conoco, Elf, Fina, Mobil, PGS, Phillips, Saga Petroleum, Schlumberger, Shell and Texaco.

### Reference

- Corrigan, D., Withers, R., Darnall, J. and Skopinski, T., 1996, Fracture mapping from azimuthal velocity analysis using 3D surface seismic data: 66th Internat. Mtg., Soc. Explor. Geophys., Expanded Abstracts, 1834-1837.
- Donati, M. and Brown, R.J., 1995, Birefringence study on 3-C/2-D: Barinas Basin (Venezuela): 65th Internat. Mtg., Soc. Explor. Geophys., Expanded Abstracts, 723-726.
- Grechka, V., and Tsvankin, I., 1996, 3-D description of normal moveout in anisotropic media: 66th Internat. Mtg., Soc. Explor. Geophys., Expanded Abstracts, 1487-1490.
- Li, X.-Y., 1997, Viability of azimuthal variation in *P*-wave moveout for fracture detection: 67th

## Fracture detection using $P$ - $P$ and $P$ - $S$ waves

- Internat. Mtg., Soc. Explor. Geophys., Expanded Abstracts, 1555-1558.
- Li, X.-Y., 1998, Azimuthal moveout analysis for fracture detection in marine streamer data: 60th EAGE Meeting, Expanded Abstracts, P-154.
- Li, X.-Y., Kühnel, T. and MacBeth, C., 1996, Mixed mode AVO response in fractured media: 66th Internat. Mtg., Soc. Explor. Geophys., Expanded Abstracts, 1822-1825.
- Lynn H.B., Simon K.M., Bates C.R., and Van Dok, R., 1996, Naturally fractured gas reservoir's seismic characterization: 66th Internat. Mtg., Soc. Explor. Geophys., Expanded Abstracts, 1360-1363.
- Mallick S., Craft K.L., Meister L.J., and Chambers R.E., 1996, Computation of principal directions of azimuthal anisotropy from  $P$ -wave seismic data: 66th Internat. Mtg., Soc. Explor. Geophys., Expanded Abstracts, 1862-1865.
- Rüger, A., 1996, Variation of  $P$ -wave reflectivity with offset and azimuth in anisotropic media: 66th Internat. Mtg., Soc. Explor. Geophys., Expanded Abstracts, 1810-1813.
- Sena, A.G., 1991, Seismic travel time equations for azimuthally anisotropic and isotropic media: Estimation of interval elastic properties: Geophysics, **56**, 2090-2101.

- Taylor, D.B., 1990, Anisecis manual: Applied Geophysical Software.
- Thomsen, L.A., 1986, Weak elastic anisotropy: Geophysics, **51**, 1954-1966.
- Tsvankin, I., 1995, Inversion of moveout velocities for horizontal transverse isotropy: 65th Internat. Mtg., Soc. Explor. Geophys., Expanded Abstracts, 735-738.

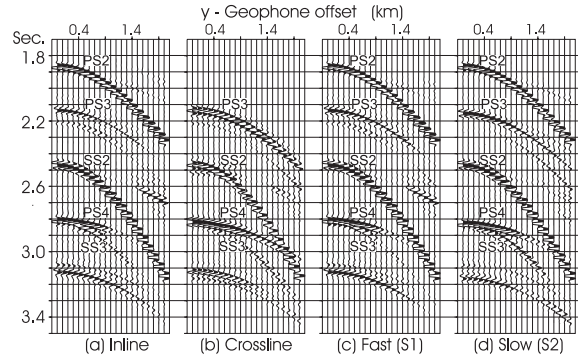


Figure 5. Inline-shooting gathers of (a) inline, (b) crossline, (c) S1 (fast  $S$ -wave) and (d) S2 (slow  $S$ -wave) components for source offset  $x_S=0$ ,  $y_{G1}=-2$  km and  $y_{GN}=1$  km with 50 m spacing. The shear-waves in (c) and (d) are clearly separated with similar forms and better continuity than those in (a) and (b).

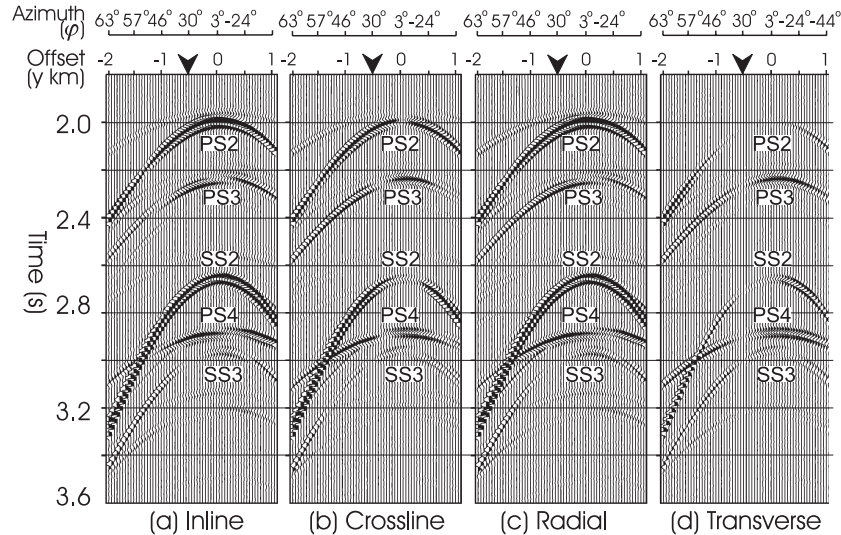


Figure 4. Azimuthal gathers of (a) inline, (b) crossline, (c) radial and (d) transverse components, calculated from the model in Figure 3 and Table 1 for source offset  $x_S=1$  km,  $y_{G1}=-2$  km and  $y_{GN}=1$  km with 50 m spacing. The triangular arrows mark the critical azimuth with a polarity reversal and amplitude minimum. Label PS2 stands for the  $P$ - $S$  conversion from interface 2, and PS3 for the conversion from interface 3, etc.